Nuclear Engineering and Design xxx (xxxx) xxx

Contents lists available at ScienceDirect

Nuclear Engineering and Design

journal homepage: www.elsevier.com/locate/nucengdes

Effect of nuclear heat caused by the ^{6}Li(n,α)T reaction on tritium containment performance of tritium production module in High-Temperature Gas-Cooled reactor for fusion reactors

Yuki Koga [a,*], Hideaki Matsuura [a], Kazunari Katayama [b], Teppei Otsuka [c], Minoru Goto [d], Shimpei Hamamoto [d], Etsuo Ishitsuka [d], Shigeaki Nakagawa [d], Kenji Tobita [e], Satoshi Konishi [f], Ryoji Hiwatari [g], Youji Someya [g], Yoshiteru Sakamoto [g]

[a] Department of Applied Quantum Physics and Nuclear Engineering, Kyushu University, 744 Motooka Nishi-ku Fukuoka-shi Fukuoka, 319-0395 Japan
[b] Department of Advanced Energy Engineering Science, Kyushu University, 6-1 Kasugakouen Kasuga-shi Fukuoka, 816-0811 Japan
[c] Department of Electrical and Electrtonic Engineering, Kindai University, 3-4-1 Kowakae, HigashiOsaka city Osaka, 577-0818 Japan
[d] Japan Atomic Energy Agency, 4002 Narita-cho Oarai-machi Higashi-Ibaraki-gun Ibaraki, 311-1393 Japan
[e] Department of Quantum Sci. Energy Eng., Tohoku University, 6-6-01-2 Aoba, Sendai City, Miyagi 980-8579, Japan
[f] Institute for Advanced Energy, Kyoto University, Gokasho, Uji, Kyoto 611-0011, Japan
[g] National Institutes for Quantum and Radiological Sci. Tech., Rokkasho, Aomori 039-3212, Japan

ARTICLE INFO

Keywords:
Fusion reactor
Tritium production
HTGR
Tritium production module
Nuclear reaction heat

ABSTRACT

Tritium is required for research and development activities for the deuterium–tritium (DT) fusion reactor and fueling the DEMOnstration Power Station (DEMO). However, tritium is a very rare nuclide and must be produced artificially. Tritium production by loading Li compounds (Li rods) into burnable poison holes of a high-temperature gas-cooled reactor (HTGR) has been proposed (H. Matsuura, et al., Nucl. Eng. Des. 243 (2012) 95–101.). Al_2O_3 and Zr are used to prevent tritium leaks. Nuclear reaction heat caused by the nuclear reaction (e.g., ^{6}Li(n,α)T reaction) can cause a spatial temperature profile in the Li rods and may change its tritium containment performance, because Al_2O_3 and Zr performance strongly depend on these temperatures. The effect of nuclear reaction heat by the ^{6}Li(n,α)T reaction on the tritium containment performance of the Li rods was evaluated by simulation. The temperatures of the Li rods for the high-temperature engineering test reactor (HTTR) and gas turbine high-temperature reactor 300 (GTHTR300) increased by 36 K and 46 K, and the leaked tritium decreased by 32% and 37% via nuclear reaction heat, respectively.

1. Introduction

To conduct research and development for the deuterium–tritium (DT) fusion reactor, tritium is required. Tritium must be produced artificially in nuclear facilities because it is a rare nuclide in nature, and deuterium can be obtained from water. Approximately 200 g of tritium are consumed per day in a fusion reactor with 1.5 GW of thermal output power. A large quantity of initial tritium is also required to start up a fusion reactor, which operates with producing tritium more than consuming tritium. It has been reported that the amount of initial tritium required for the DEMOnstration Power Station (DEMO) is several 100 g - approximately 27 kg (Hiwatari, 2018; Asaoka et al., 1996). In addition, ≥100 g of tritium is required for an engineering test before DEMO reactors are built. The tritium supplied to the International Thermonuclear Experimental Reactor (ITER) is produced from Canadian Deuterium Uranium reactors (CANDU) in Canada (Gierszewski, 1989). However, it has not been clarified how the tritium for the first DEMO reactors, particularly those in Japan, will be supplied. Thus, we have proposed a tritium production method using a high-temperature gas-cooled reactor (HTGR) (Matsuura et al., 2012) by loading tritium production modules containing a Li compound as a burnable poison (BP). The HTGR is primarily composed of graphite (moderator) and He (coolant), which are chemically stable and do not react with the Li compound. Furthermore, the required amount of Li compound can be loaded without ^{6}Li concentration because the HTGR core size is larger than other types of fission reactors, such as the pressurized water reactor

* Corresponding author.
E-mail address: koga_yuki@nucl.kyushu-u.ac.jp (Y. Koga).

https://doi.org/10.1016/j.nucengdes.2021.111584
Received 20 June 2021; Received in revised form 15 November 2021; Accepted 20 November 2021

(PWR) and boiling water reactor (BWR). Normal BP is cylindrical solid B_4C, so with that same form, the module can be loaded without significantly changing the original core design from the standard one. We assume that in the module the Li compound and Zr (tritium absorber) are sealed in cylindrical Al_2O_3 (Matsuura et al., 2019). This module is an Li rod, which produces tritium, while Zr absorbs tritium during the operation. The tritium must be contained so that leaking into the coolant is maintained as low as possible. The tritium leakage rate was evaluated to be below 1% at 800 K by performing numerical simulations of the Li rods without Zr (Nakaya et al., 2015). It was supposed that the gas turbine high-temperature reactor 300 (GTHTR300) (Nakata, 2002) produced 400–600 g of tritium in six months on the simulation (Nakaya et al., 2015). However, most of produced tritium might leak with the increased Al_2O_3 hydrogen permeability (Katayama et al., 2015), if the normal outlet temperature is supposed to be 1,070 K–1,170 K to maintain thermal efficiency. Accordingly, we considered using Zr as a tritium absorber and its shape for the Li rods. Fig. 1 shows the current design of the Li rods with Zr considered for efficient tritium absorption (Matsuura et al., 2019). It has been reported that tritium absorption performance of Zr worsens during oxidation and a Ni coating can be applied to prevent this (Matsuura et al., 2019). Moreover, Zr pebbles can be used for large absorption areas. It was expected that Li rods with Zr can reduce tritium leakage and contain enough tritium if the deterioration of Ni-coated Zr is minimized during oxidation (Matsuura et al., 2019). We have been advancing an irradiation test plan for the high-temperature engineering test reactor (HTTR) (Saito, 1994) to confirm the Li rod and Ni-coated Zr performance as well as demonstrate the HTGR's tritium production (Koga et al., 2018). The HTTR is an experimental HTGR with 30 MW of thermal output owned by the Japan Atomic Energy Agency (JAEA). The structure of Li irradiation units has been investigated for feasible irradiation tests. So far, we have conducted hydrogen absorption experiments to measure the hydrogen absorption performance of Zr using Zr powder (Izumino et al., 2018), Zr cylinders (Matsuura et al., 2019; Matsuura, 2021), and one-side sealed Zr pipes (Katayama et al., 2018) However, the tritium absorption performance of Zr in Li rods inserted into the HTGR has not been measured yet. We have developed an analysis model for tritium production and containment in the GTHTR300 and HTTR (Matsuura, 2021).

Energy is generated per the following reaction when tritium is produced

$$6Li + n \rightarrow T + \alpha + 4.8\text{MeV}$$

This energy appears as kinetic energy in generated particles and changes to thermal energy via collisions between particles and other atoms. Tritium and α particles remain in the Li rods so that the temperature in the rods increases, and the temperature distribution appears via the temperature difference compared to its surroundings. The amount of produced tritium in the GTHTR300 is more than that in the HTTR due to the differences in reactor sizes, loaded amount of ^{6}Li, and thermal outputs for these reactors. If about 193 g (6,550 g) of ^{6}Li is loaded into the HTTR (GTHTR300) and 30 g (800 g) of tritium is produced in a year, the nuclear reaction heat of Li rods is estimated to be 300 W (1,800 W) considering only the ^{6}Li(n,α)T reaction. The results of this experiment imply that the tritium containment performance of the Al_2O_3 layer deteriorated as the temperature increased (Katayama et al., 2015). Meanwhile, the hydrogen absorption performance using Zr cylinders at 1,170 K and 1,120 K shows that the hydrogen absorption speed at 1,170 K is faster than that at 1,120 K (Matsuura et al., 2019), implying that the tritium absorption performance of Zr is better at higher temperatures. These evaluations were conducted under the assumptions that Li rods do not have a temperature distribution and that the temperature was the assumed temperature or coolant temperature (Matsuura et al., 2012, 2019; Koga et al., 2018; Matsuura et al., 2012; Nagasumi, 2017).

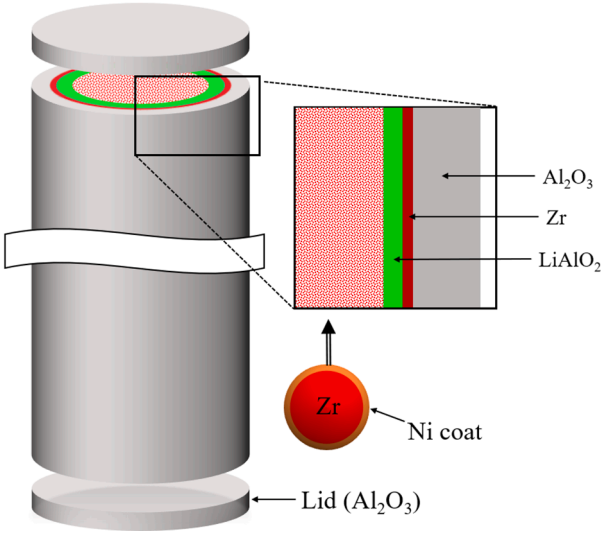

Fig. 1. Schematic diagram of Li rods.

In research on fusion reactor blankets, a coolant system has been designed by fluid dynamics analysis based on the coolant conditions for PWR. Previous studies in the blanket system have shown the importance of nuclear reaction heat on fusion and nuclear reactors. In the evaluation, it was assumed that the JA DEMO and temperature of the inlet coolant water were 568 K, and the maximum temperatures of the Li/Be mixed pebble region and the structural material were evaluated as 1,119 K and 817 K, respectively, and satisfied the permissible range (Someya, 2019). The maximum fuel temperature in the HTTR is limited to 1,768 K for safety, and the temperature was calculated to be at a maximum of 1,765 K in normal operation via simulation (Maruyama, 1994). Moreover, we have evaluated reactor temperature and temperature coefficient reactivity by simulation to confirm the nuclear and thermal feasibility of the HTGR loaded with Li rods (Goto, 2018). The maximum fuel temperature was 1,746 K, i.e., lower than the limit, so the $LiAlO_2$ would not melt (Goto, 2018). Now, it is necessary to confirm the temperature distribution in the Li rods via the nuclear reaction heat and evaluate the thermal effects on the rods' tritium containment performance. The amount of leaked tritium may change as the temperature increases due to the reaction heat since a substantial amount of Zr is loaded into the Li rods.

In this study, we evaluate the effects of nuclear reaction heat by the ^{6}Li(n,α)T reaction on the tritium containment performance of the Li rods for the HTTR and GTHTR300 and compare the changes in the amount of leaked tritium with previous evaluations in which the nuclear reaction heat was not considered.

2. Calculation model

2.1. Li rod structure and HTGR designs

The schematic diagram of the HTTR and GTHTR300 cores are shown in Figs. 2 and 3. The HTTR core consists of 30 fuel columns and seven control rod guide columns surrounded with permanent/replaceable reflector columns and nine control guide columns. There are five core layers and four reflector layers. The core is 2.9 m in height and 2.3 m in equivalent diameter. The block is 580-mm high and 360-mm wide across the flats. The fuel blocks contain either 31 or 33 fuel rods and three BP holes. The GTHTR300 is an HTGR design created by the JAEA that has 600 MW of thermal output. Its core is ring-shaped, consisting of 90 fuel columns, 30 control rod guide columns, and 46 replaceable reflector columns. It is surrounded with permanent reflector columns both inside and outside. There are eight core layers and two reflector layers. The core is 8 m in height and about 5.6 m in diameter. The block is 1,000-mm high and 405-mm wide across the flats. The fuel blocks

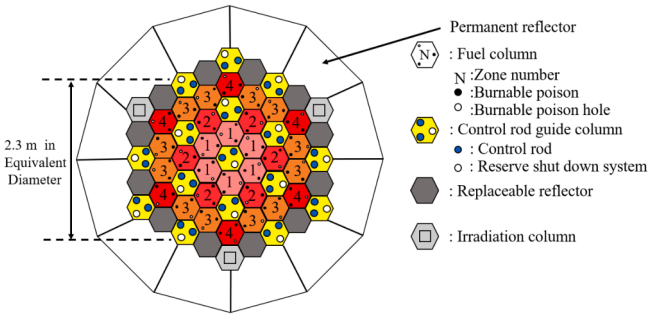

Fig. 2. Schematic diagram of the HTTR core. The HTTR consists of five core layers.

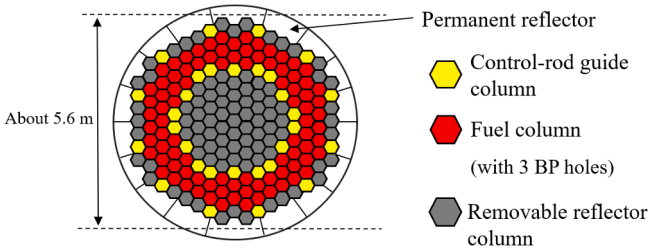

Fig. 3. Schematic diagram of the GTHTR300 core. The GTHTR300 consists of eight core layers.

contain 57 fuel rods and three BP holes. The moderator temperature of the HTTR is in the range of 900 K–1,280 K.

Figs. 4 and 5 show the Li rod designs proposed for both reactors currently. The Li rods for the HTTR are 450 mm in height and 14 mm in diameter. They consist of a hollow portion, Li compound ($LiAlO_2$) with 85% theoretical density (Kawamura et al., 1992), Zr layer/pebbles, and Al_2O_3 layer. The concentration of ^6Li in the $LiAlO_2$ was set at its natural abundance. The Li rods for the GTHTR300 were 1,000 mm in height and 44 mm in diameter, and their structure was the same as that of the HTTR Li rods. In this simulation, Zr pebbles were inserted with 60% hollow portion volume into each Li rod.

2.2. Nuclear calculation

To evaluate the amount of tritium produced in the Li rods and effective multiplication factor (k_{eff}), we conducted a nuclear calculation

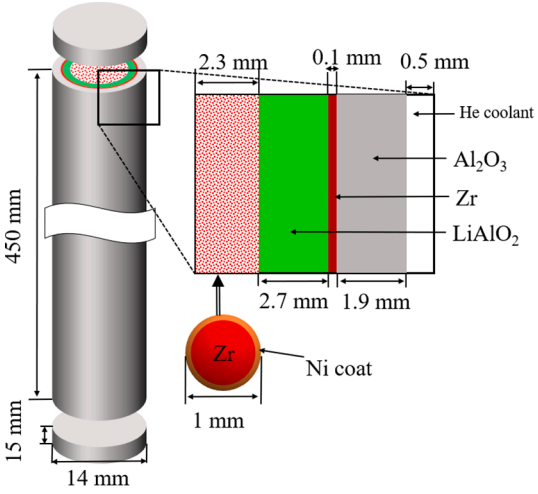

Fig. 4. Schematic diagram of Li rods for the HTTR. The Zr layer is Ni-coated. The $LiAlO_2$ layer has 85% of theoretical density.

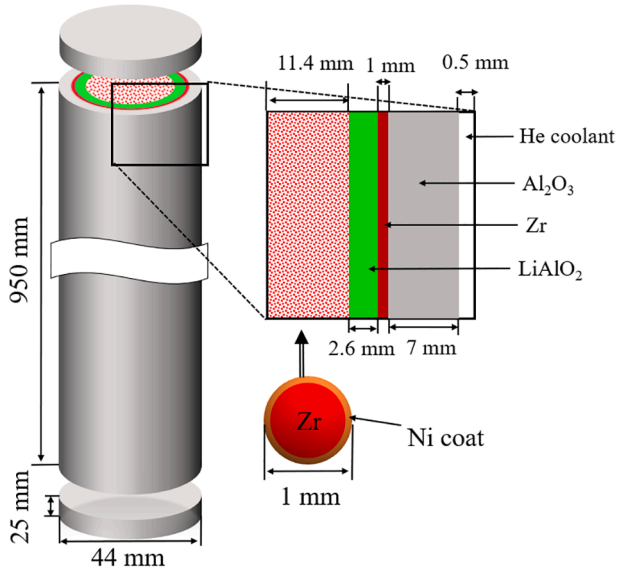

Fig. 5. Schematic diagram of Li rods for the GTHTR300. The characteristics of the Zr and $LiAlO_2$ layer are same to Fig. 4.

using the continuous-energy Monte Carlo transport code MVP-BURN (Nagaya, 2017; Okumura et al., 2000) with the Japanese Evaluated Nuclear Data Library-4.0 (JENDL-4.0) (Shibata, 2011). We assumed the HTTR and GTHTR300 core system with Li rods loaded into all BP holes for a 360-day operation period. The average moderator temperature of the Li rods for the HTTR was set at 1,140 K, and that for the GTHTR300 was set at 1,190 K. It was assumed that all control rods were pulled up on these simulations. Considering the actual reactor operation, the k_{eff} on day 360 was supposed to be over 1.02. The time steps for the burn-up simulation were set as 0, 1, 5, 30, 60, 120, 180, and 360 days. The thermal outputs for the HTTR and GTHTR were set at 30 and 600 MW, respectively, throughout the operation. Moreover, six million neutron particles were generated in these simulations so that the statistical error was guaranteed to be less than 0.1% for the k_{eff} and reaction rates on nuclides in fuel and Li rods.

2.3. Nuclear reaction heat generation model

The nuclear reaction heat of only the $^6Li(n,\alpha)T$ reaction was considered here. The nuclear reaction heat was converted from the tritium produced in an Li rod as follows:

$$q''' = \frac{n}{V_{Li} N_A} Q \tag{1}$$

where q‴, n, V_{Li}, N_A, and Q are the nuclear reaction heat per volume (W/m^3), tritium production rate by an Li rod (mol/s), volume of the $LiAlO_2$ layer (m^3), Avogadro's constant, and Q value of the $^6Li(n,\alpha)T$ reaction energy (J), respectively. A stationary heat diffusion equation was used in the cylindrical coordinate with q‴, and the temperature distribution of an Li rod was evaluated for the radius direction:

$$\frac{1}{r}\frac{\partial}{\partial r}\left(kr\frac{\partial T}{\partial r}\right) + q''' = 0 \tag{2}$$

where r, k, and T are the distance of the radius direction (m), thermal conductivity (W/m K) of each layer at 1,073 K, and temperature (K), respectively. It was assumed that the Li rods and He gas in the fuel block were sealed by graphite dowel pins as the design data shows. Therefore, the existence of He gas between the Li rods and fuel block was considered. The applied thermal conductivity values of each layer are shown in Table 1 (Schulz and Wedemeyer, 1986; Fink and Leibowitz, 1995; Auerkari, 1996; Faubert and Springer, 1973; Powell, 1965). The thermal conductivity of Zr was smaller than that of Ni so that we adopted pure-Zr

Table 1
Thermal conductivity of Li rod layers.

	$LiAlO_2$	Zr	Al_2O_3	He	Ni
Thermal conductivity(W/m K)	3.96	22.8	6.34	0.375	73.7

thermal conductivity for the Ni-coated Zr.

2.4. Tritium absorption model for Zr

We applied the hydrogen diffusivity and solubility coefficient for Zr measured by the outer Zr pipe in a previous study[1] (Katayama et al., 2018). Diffusion calculations by the diffusion equation and Sieverts' law were conducted to evaluate the amount of tritium absorbed into the Zr. The Zr pebbles and Zr layer were assumed to have converted to a Zr cylinder with the same surface area. The diffusion equation in a cylinder coordinate system was as follows:

$$\frac{\partial C_{Zr}(t,r_{Zt})}{\partial t} = \frac{D_{Zr}}{r_{Zr}}\frac{\partial}{\partial r_{Zt}}\left(r_{Zr}\frac{\partial C_{Zr}(t,r_{Zt})}{\partial r_{Zr}}\right) \tag{3}$$

where C_{Zr} , t, D_{Zr} , and r_{Zt} are the tritium concentration in Zr (mol/m^3), time (s), the diffusion coefficient of the Zr (m^2/s), and distance of the radius direction (m), respectively. This equation was used to calculate the tritium concentration distribution in the Zr. Sieverts' law was used as the boundary condition of the Zr surface.

$$C_{Zr0} = S_{Zr}\sqrt{P} \tag{4}$$

where C_{Zr0} , S_{Zr} , and P are the tritium concentration in the Zr surface (mol/m^3), solubility coefficient of the Zr (mol/m^3/$Pa^{1/2}$), and tritium partial pressure (Pa), respectively. It has been confirmed that tritium absorption phenomena by Zr are consistent with Sieverts' law in the past experiments (Matsuura et al., 2019, 2021; Izumino et al., 2018; Katayama et al., 2018). Then, C_{Zr} was integrated in the Zr volume and differentiated in time to evaluate the amount of tritium absorbed in the Zr, as follows:

$$J_{Zr} = -\frac{\partial}{\partial t}\int_{V_{Zr}} C_{Zr}(t,r)d^3r \tag{5}$$

where J_{Zr} and V_{Zr} are the tritium flux from the surface of Zr (mol/s) and the volume of the assumed Zr cylinder (m^3), respectively, while D_{Zr} and S_{Zr} were cited from Katayama et al. (2018). The value of S_{Zr} was obtained from D_{Zr} and the hydrogen permeability. It was assumed that the coefficient functions were held for any temperature. The temperature of the center of any Li rod was adapted to the functions. Furthermore, D_{Zr} was reduced by 1/2,000 to consider the reported influence of the Ni coating (Otsuka, et al., 2020).

2.5. Tritium leakage model for Al_2O_3 layer

To evaluate the tritium leakage, we used this tritium diffusion equation in the cylindrical coordinate:

$$\frac{\partial C_{Al}(t,r_{Al})}{\partial t} = \frac{D_{Al}}{r_{Al}}\frac{\partial}{\partial r_{Al}}\left(r_{Al}\frac{\partial C_{Al}(t,r_{Al})}{\partial r_{Al}}\right) \tag{6}$$

where C_{Al} , t, D_{Al} , and r_{Al} are tritium concentration in the Al_2O_3 layer (mol/m^3), time (s), diffusion coefficient of the Al_2O_3 layer (m^2/s), and distance of the radius direction (m), respectively. The temperature at the inner boundary was used for the D_{Al} value as a conservative evaluation. Sieverts' law was used as the boundary condition just as in the Zr tritium absorption model:

$$C_{Al0} = S_{Al}\sqrt{P} \tag{7}$$

where C_{Al0} , S_{Al} , and P are the tritium concentration in the inner surface of the Al_2O_3 layer (mol/m^3), the solubility coefficient of the Al_2O_3 layer (mol/m^3/$Pa^{1/2}$) and partial pressure in the hollow portion (Pa), respectively. Sieverts' law can be adopted for Al_2O_3 layer because the gas diffused by atomic form in the high density Al_2O_3 tube in the experiment (Katayama et al., 2015). The inner boundary temperature of the Al_2O_3 layer was used for the S_{Al} and D_{Al} values for conservative calculation. The D_{Al} and S_{Al} values for Al_2O_3 used in **Eqs. (6) and (7)** were cited from Katayama, K. et al. (Katayama et al., 2015), and it was assumed that their temperature functions were also held for any temperature. To calculate the amount of permeated tritium in the inner (outer) surface of the Al_2O_3 layer, Fick's law was used:

$$J_{in,out} = -A_{in,out}D_{Al}\left.\frac{\partial C_{Al}}{\partial r_{Al}}\right|_{in,out} \tag{8}$$

where $J_{in}(J_{out})$ and $A_{in}(A_{out})$ are the tritium flux from the inner surface of the Al_2O_3 layer (the inner Al_2O_3 layer) to the inner Al_2O_3 layer (the outer surface of the Al_2O_3 layer) (mol/s) and the inner (outer) surface area of the Al_2O_3 layer (m^2), respectively. The tritium in the outer surface of the Al_2O_3 layer was assumed to leak into the He coolant immediately. Finally, **Eqs. (5)–(8)** were united with the tritium balance equation shown below to evaluate the tritium absorption and leakage:

$$\frac{dP}{dt} = \frac{GRT}{V_{hp+Li(15)}} + \frac{J_{Zr}RT}{V_{hp+Li(15)}} + \frac{J_{in}RT}{V_{hp+Li(15)}} \tag{9}$$

where G, R, and $V_{hp+Li(15)}$ are the tritium molecule generation speed (mol/s), gas constant (J/K mol), and volume of the hollow portion and void of the $LiAlO_2$ layer in an Li rod (m^3), respectively. We ignored the anti-permeation property of Zr that prevented the tritium from permeating into the Al_2O_3 layer for the conservative evaluation. Finally, Fig. 6 shows the tritium leakage model using **Eq. (9)**. The tritium produced in the $LiAlO_2$ quickly entered the hollow portion, and a portion of it was absorbed by the Zr. The tritium diffused into the Al_2O_3 layers and then leaked into the He region (tritium concentration: C = 0).

3. Results and discussion

3.1. Tritium produced in the HTGRs and calorific value of the Li rods

Fig. 7 shows the cumulative amount of tritium produced and the k_{eff} over 360 days of operation for the HTTR and GTHTR300. The amount of tritium produced and the k_{eff} values after 360 days of operation for the HTTR (GTHTR300) were 30.4 g/y (807.3 g/y) and 1.028 (1.020). The

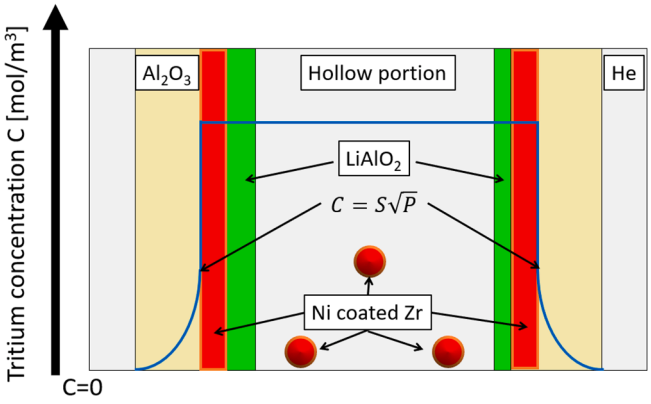

Fig. 6. Schematic diagram of the tritium leak model in the Li rod. The blue curve shows the tritium concentration. (For interpretation of the references to colour in this figure legend, the reader is referred to the web version of this article.)

[1] The diffusivity coefficient was cited from the study. The permeability coefficient is the product of diffusivity and solubility coefficient so that the solubility coefficient converted from it and the permeability coefficient.

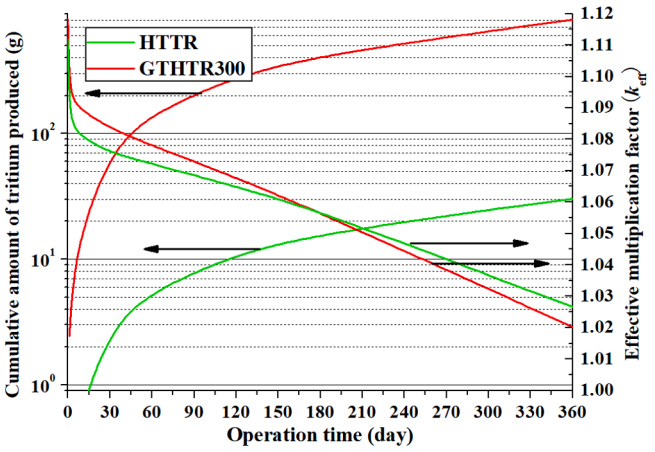

Fig. 7. The cumulative amount of tritium produced, and the k_{eff} value throughout the 360 days of operation for the HTTR and GTHTR300.

k_{eff} for the GTHTR300 decreased more rapidly than that of the HTTR during the operation. The produced tritium was used to evaluate the calorific values of the Li rods for both reactors. The tritium production speed per one Li rod for the HTTR (GTHTR300) was 2.17×10^{-9} g/s (1.20×10^{-8} g/s). The Q value of the ^{6}Li(n,α)T nuclear reaction energy is 4.8 MeV, so the nuclear reaction heat for one Li rod for the HTTR (GTHTR300) was 333 W (1,845 W). The volume of the $LiAl_2O$ layer in the cylinder-shaped V_{Li} for the HTTR (GTHTR300) was 2.79×10^{-5} m^3 (1.97×10^{-4} m^3), and the ^{6}Li atoms were assumed to be uniform in the $LiAl_2O$ layer. Using **Eq. (1)**, the nuclear reaction heat per volume (W/m^3) for the HTTR (GTHTR300) was evaluated as 1.20×10^{7} W/m^3 (9.36×10^{6} W/m^3).

3.2. Evaluation of the nuclear reaction heat and its effect

Before the evaluation of the effect by nuclear reaction heat, we compared the accuracy of the tritium leakage calculation to the accurate evaluation (Matsuura, 2021) and found that the accuracy was acceptable.

We evaluated the radial profile of the temperature in the Li rods for the HTTR (Fig. 8) using the values of the nuclear reaction heat shown in Section 3.1 and **Eq. (2)**. If the nuclear reaction heat was not considered, the distribution was constant at 1,140 K (moderator temperature). When considering the reaction heat, the temperature increased. The maximum temperature was 1,176 K (a 36 K increase) in the hollow portion and Zr pebble regions, and the temperature dropped in the outer region. The temperature distribution was always constant in the hollow and Zr pebble regions at steady state regardless of effective thermal conductivity by any material forms. This is derived from **Eq. (2)**. If the effective thermal conductivity reduces in $LiAlO_2$, Zr, and Al_2O_3 layer by irradiation, temperature will increase there. The temperature dropped the most in the He region because the He thermal conductivity was low and worked as a heat gap. The amount of tritium produced by the Li rods for the HTTR and the leaked tritium with/without the reaction heat after 360 days of operation are shown in Fig. 9. If the reaction heat was not considered, the amount of leaked tritium was 5.03×10^{-1} g, and the leakage rate was 1.66%. When considering the reaction heat, the amount of leaked tritium was 3.43×10^{-1} g, and the leakage rate was 1.13%. Thus, there was a 31.8% decrease in the leaked tritium via the reaction heat.

The temperature distribution in the Li rods for the GTHTR300 was evaluated in the same way as for the HTTR. Fig. 10 shows the temperature distribution. If the reaction heat was not considered, the distribution was constant at 1,190 K. The maximum temperature was 1,236 K (a 46 K increase) in the hollow portion and Zr pebble regions. The higher reaction heat simply increased the maximum temperature. Large materials have high heat retention, and thick layers generally retain heat. Therefore, it was considered that the larger size of the Li rods and thicker Al_2O_3 layer caused the higher temperature increase. Fig. 11 shows the cumulative tritium produced and leaked from the Li rods for the GTHTR300 with/without reaction heat after a one-year operation period. The amount of leaked tritium was 2.67×10^{-1} g, and the leak rate was 3.31×10^{-2} % when the reaction heat was not considered. The tritium leakage of the Li rods for the GTHTR300 decreased even more than that for the HTTR by loading more Zr, although the GTHTR300 produced more tritium. Considering the reaction heat, the amount of leaked tritium was 1.68×10^{-1} g, and the leak rate was 2.08×10^{-2} %. There was a 37.1% decrease in the leaked tritium via the reaction heat, higher than that for the HTTR. This was because the temperature increase caused by the nuclear reaction heat for the GTHTR300 was higher, and the Zr performance was better. These results show that the amount of leaked tritium was decreased by the reaction heat for the GTHTR300 as well.

To confirm roughly the time that the temperature distributions reach steady state, we evaluated the time that the Li rods reach maximum temperature when heat does not transfer outside the Li rods. Table 2

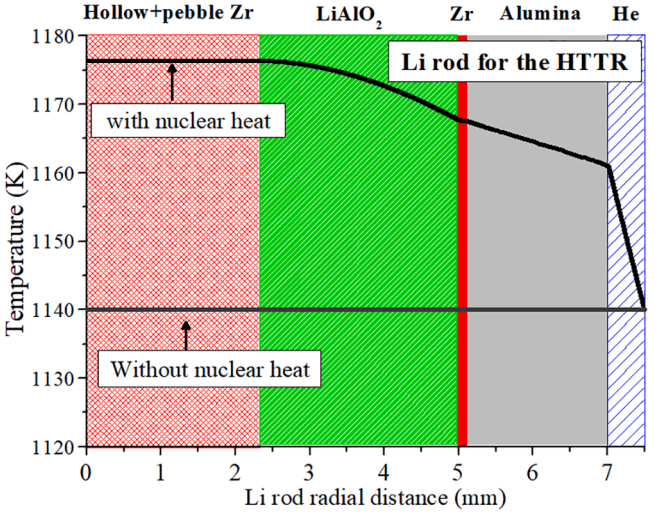

Fig. 8. Temperature distribution of the Li rods for the HTTR. The nuclear reaction heat was 333 W. The maximum temperature was 1,176 K in the hollow and Zr pebble region.

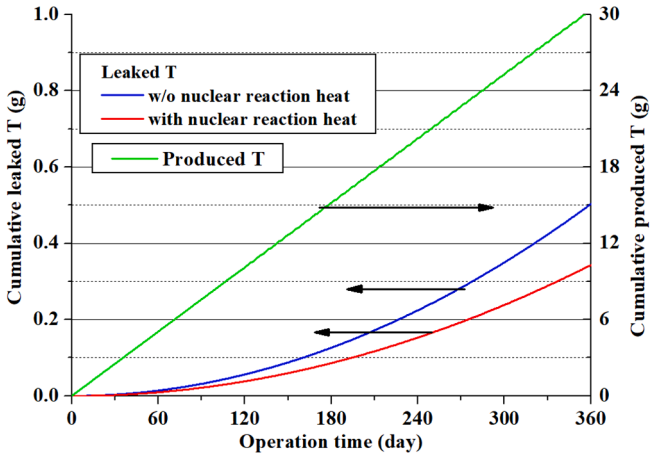

Fig. 9. The amount of tritium produced and leaked by the Li rods for the HTTR with and without the nuclear reaction heat throughout the 360 days of operation. There was a 31.8% decrease in the leaked tritium via the reaction heat.

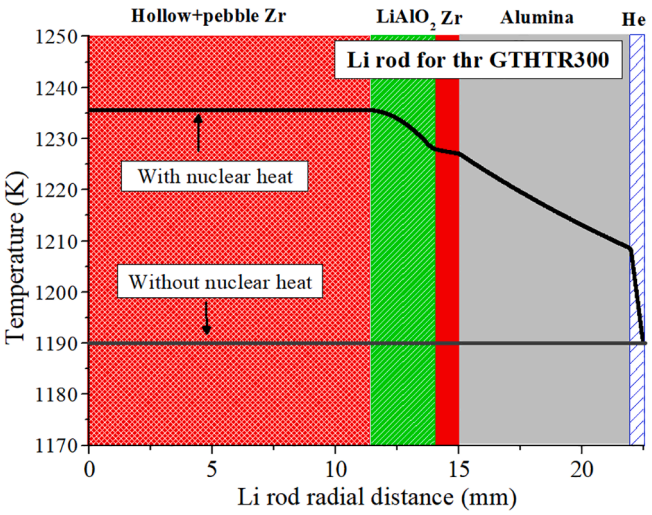

Fig. 10. Temperature distribution of the Li rods for the GTHTR300. The nuclear reaction heat was 1,845 W. The maximum temperature was 1,236 K in the hollow and Zr pebble region.

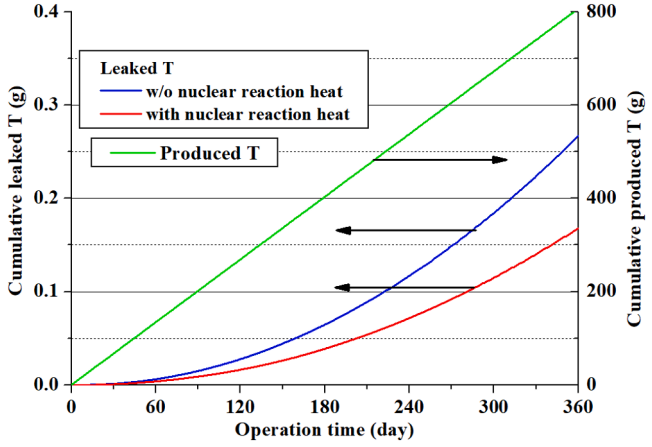

Fig. 11. The amount of tritium produced and leaked by the Li rods for the GTHTR300 with and without the nuclear reaction heat throughout the 360 days of operation. There was a 37.1% decrease in the leaked tritium via the reaction heat.

Table 2
Molar heat capacity of Li rod layers. Value for Al_2O_3 was converted from specific heat capacity.

	$LiAlO_2$	Zr	Al_2O_3	He
Molar heat capacity(J/mol K)	102.7	33.5	123.1	20.8

shows molar heat capacity values of each layer (Fink and Leibowitz, 1995; Auerkari, 1996; Chase, 1998; Kleykamp, 1999). The heat capacity of Li rods for the HTTR (GTHTR300) was calculated to be about 295 (5652) J/K. If the temperature of the Li rods for the HTTR (GTHTR300) increase by 36 (46) K, the required time was 32 (141) s. Therefore, the period during transient state was shorter than the operation time so that the influence of transient state could be ignored.

3.3. Analysis of the effect of nuclear reaction heat

We analyzed the results of Section 3.2. Fig. 12 shows the tritium leakage rate and partial pressure of the Li rods for the HTTR after 360 days of operation at 770 K–1,176 K with only the Al_2O_3 layer as the

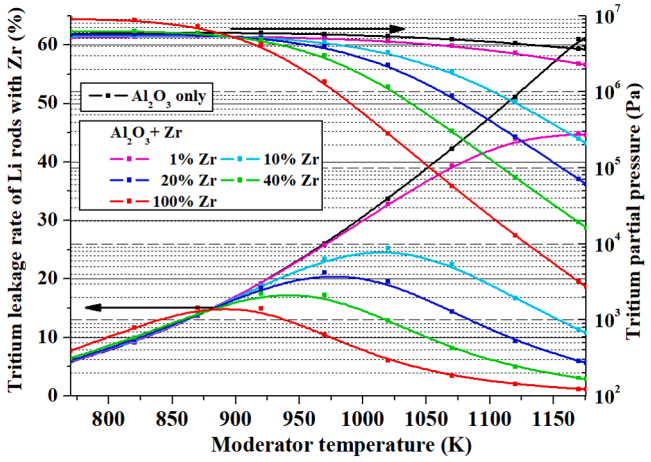

Fig. 12. Tritium leakage rate of the Li rods and tritium partial pressure for the HTTR after 360 days of operation at 770– 1,176 K with only Al_2O_3 layer as tritium containment function or Zr. The percentage of Zr was the Zr loading rate of the Zr layer and pebbles. When it was 100%, the amount of loaded Zr in the Li rods is the same as those evaluated in Section 3.2.

tritium containment function or with Zr. The percentage of Zr was the Zr loading rate of Zr layer and pebbles. When it is 100%, the amount of loaded Zr in the Li rods is the same as those evaluated in Section 3.2. Fig. 13 shows the tritium absorption rate of Zr per produced tritium as tritium absorption performance at 770 K–1,176 K based on the evaluation of Fig. 12. The thickness of the Al_2O_3 layer was 2.0 mm when the Zr layer was not considered. When only the Al_2O_3 layer was used for the Li rods, the tritium leakage rate increased due to the increase in moderator temperature. This is because Al_2O_3 hydrogen permeability is directly proportional to the temperature (Katayama et al., 2015). When Zr was considered, the tritium adsorption rate increased with an increase in temperature since Zr hydrogen permeability is also proportional to the temperature (Katayama et al., 2018). The tritium leakage rate increased at peak temperatures from the minimum temperature due to the increase in temperature. This is because the tritium absorption performance of Zr under the peak temperature was lower than the tritium containment performance of the Al_2O_3 layer deteriorated by the temperature increase. The tritium leakage rate and partial pressure decreased over the peak temperature due to the increase in temperature. This is because the tritium absorption of Zr performs better than tritium

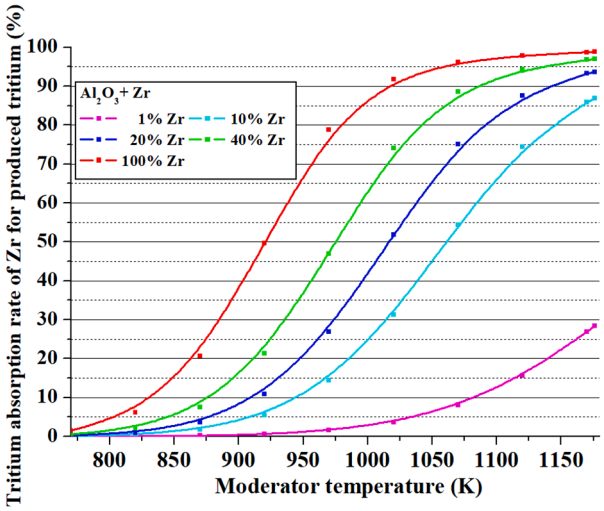

Fig. 13. Tritium absorption rate of Zr per produced tritium at 770–1,176 K based on the evaluation of Fig. 12.

containment of the Al_2O_3 layer. The peak temperature increased when the Zr loading rate decreased from 100% because the tritium absorption rate of Zr was proportional to the Zr loading rate.

Overall, the leaked tritium from the Li rods mainly decreased with the temperature increase of Li rods caused by the nuclear reaction heat. It is expected that the change in tritium leakage from the Li rods for the HTTR caused by the nuclear reaction heat is almost consistent with Fig. 12 since the influence of the temperature difference between the Al_2O_3 layer and Zr shown in Fig. 8 is small. The case of the GTHTR300 has similar results. The leaked tritium from the Li rods for the HTTR decreases at over 900 K by the nuclear reaction heat when the Zr loading rate is 100%.

4. Concluding remarks

We evaluated the effect of the nuclear reaction heat from the ^{6}Li(n,α)T reaction on the tritium containment performance of Li rods via simulation. The temperature of the Li rods for the HTTR (GTHTR300) increased by 36 K (46 K) in the hollow portions and Zr pebble regions via the nuclear reaction heat of the ^{6}Li(n,α)T reaction, and the amount of leaked tritium decreased by 31.8% (37.1%) for the temperature increase. This is because the tritium absorption performance of the Zr improved more than the deteriorated tritium containment performance of the Al_2O_3 layer. Considering the effect of the moderator temperature, the nuclear reaction heat would decrease the tritium leakage under only high-temperature operation in the HTGR (e.g., over 900 K for the HTTR). If the He coolant was circulated in the region where the Li rods were loaded, the tritium leakage could decrease even further due to the cooling in the Al_2O_3 layer.

Currently, hydrogen absorption experiments using Ni-coated Zr have yet to be completed to measure the hydrogen absorption performance. These experiments must be completed to verify this study. We expect that tritium can be rapidly absorbed by Ni-coated Zr at high temperatures.

Only the ^{6}Li(n,α)T reaction was considered here, but other nuclear reactions in Li rods can occur by neutron irradiation. For example, ^{28}Al atoms are produced by neutron reactions in the Al_2O_3 layer and have strong radioactivity for their short half time, which may change the temperature distribution. Therefore, other reactions must be considered to evaluate their tritium containment performance. In addition, an experiment using an Li rod test unit with a heater should be conducted to confirm the effects of reaction heat on the tritium containment performance.

The temperature distribution and tritium containment performance for the Li rods can be influenced by the interaction of each layer of materials with the neutron flux and irradiation damage. It was reported that hydrogen diffusion was retarded for tungsten because of the trapping effect caused by radiation defects (Hatano et al., 2013). However, it was also reported that hydrogen diffusion was enhanced by irradiation for Al_2O_3 (Macaulay-Newcombe and Thompson, 1998). Regarding thermal conductivity, more defects and vacancies were observed in $LiAlO_2$ by neutron irradiation (Devaraj, 2021) so that thermal conductivity may decrease. The influence of irradiation has not been well understood at present. However, due to the short operation period for the tritium production (360 days) and low neutron flux in the HTGR, serious problems may not occur via irradiation. We should conduct an irradiation test in the HTTR to check the influence of neutron irradiation.

CRediT authorship contribution statement

Yuki Koga: Conceptualization, Methodology, Software, Writing – original draft, Writing – review & editing. **Hideaki Matsuura:** Conceptualization, Supervision, Project administration, Funding acquisition, Validation, Writing – review & editing. **Kazunari Katayama:** Validation, Writing – review & editing. **Teppei Otsuka:** Validation, Writing – review & editing. **Minoru Goto:** Validation, Writing – review & editing. **Shimpei Hamamoto:** Validation, Writing – review & editing. **Etsuo Ishitsuka:** Validation, Writing – review & editing. **Shigeaki Nakagawa:** Validation, Writing – review & editing. **Kenji Tobita:** Validation, Writing – review & editing. **Satoshi Konishi:** Validation, Writing – review & editing. **Ryoji Hiwatari:** Validation, Writing – review & editing. **Youji Someya:** Validation, Writing – review & editing. **Yoshiteru Sakamoto:** Validation, Writing – review & editing.

Declaration of Competing Interest

The authors declare that they have no known competing financial interests or personal relationships that could have appeared to influence the work reported in this paper.

Acknowledgments

This work was supported by JSPS (Japan Society for the Promotion of Science) KAKENHI Grant-in-Aid for Scientific Research (B) JP18H01200 and JP21H01065, and cooperative program with BA (The Joint Implementation of the Broader Approach Activities in the Field of Fusion Energy Research) reactor design team in Japan.

References

R. Hiwatari, Research frontier of tritium for fusion reactor -toward the Demo reactor- (2); Basic concept of tritium fuel balance required for DEMO, J Atomic Energy Society Japan [in Japanese] **60** (8) (2018) 52.

Asaoka, Y., Okano, K., Yoshida, T., Tomabechi, K., 1996. Requirements of Tritium Breeding Ratio for Early Fusion Power Reactors. Fusion Tech. 30 (3P2A), 853–863.

Gierszewski, P., 1989. Tritium supply for near-term fusion devices. Fusion Eng. Des. 10, 399–403.

Matsuura, H., Kouchi, S., Nakaya, H., Yasumoto, T., Nakao, Y., Shimakawa, S., Goto, M., Nakagawa, S., Nishikawa, M., 2012. Performance of high-temperature gas-cooled reactor as a tritium production device for fusion reactors. Nucl. Eng. Des. 243, 95–101.

Matsuura, H., Okamoto, R., Koga, Y., Suganuma, T., Katayama, K., Otsuka, T., Goto, M., Nakagawa, S., Ishitsuka, E., Tobita, K., 2019. Li-rod structure in high-temperature gas-cooled reactor as a tritium production device for fusion reactors. Fusion Eng. Des. 146, 1077–1081.

Nakaya, H., Matsuura, H., Katayama, K., Goto, M., Nakagawa, S., 2015. Study on a method for loading a Li compound to produce tritium using high-temperature gas-cooled reactor. Nucl. Eng. Des. 292, 277–282.

T. Nakata, et al., Nuclear Design of the Gas Turbine High Temperature Reactor (GTHTR300), JAERI-Tech (2002) 2002-066.

Katayama, K., Ushida, H., Matsuura, H., Fukada, S., Goto, M., Nakagawa, S., 2015. Evaluation of Tritium Confinement Performance of Alumina and Zirconium for Tritium Production in a High-Temperature Gas-Cooled Reactor for Fusion Reactors. Fusion Sci. Tech. 68 (3), 662–668.

S. Saito, et al., Design of High Temperature Engineering Test Reactor, JAERI-1332 (1994).

Koga, Y., Matsuura, H., Ida, Y., Okamoto, R., Katayama, K., Otsuka, T., Goto, M., Nakagawa, S., Nagasumi, S., Ishitsuka, E., Shimazaki, Y., 2018. Study on lithium rod test module and irradiation method for tritium production using high temperature gas-cooled reactor. Fusion Eng. Des. 136, 587–591.

Izumino, J., Katayama, K., Matsuura, H., Fukada, S., 2018. Study on hydrogen absorption in Zr powder used for tritium confinement in a production system of tritium for fusion reactors with a high-temperature gas-cooled reactor. Nucl. Mat. Energy 17, 289–294.

Matsuura, H., et al., 2021. The T-containment properties of a Zr-containing Li rod in a high-temperature gas-cooled reactor as a T production device for fusion reactors. Fusion Eng. Des. 169, 112441.

Katayama, K., Izumino, J., Matsuura, H., Fukada, S., 2018. Evaluation of hydrogen permeation rate through zirconium pipe. Nucl. Mat. Energy. 16, 12–18.

Nagasumi, S., et al., 2017. Study on Tritium Production Using a High-Temperature Gas-Cooled Reactor for Fusion Reactors: Evaluation of Tritium Outflow by Non-Equilibrium Diffusion Simulations Fusion Sci. Tech. 72, 753–759.

Y. Someya, et al., Development of water-cooled blanket concept with pressure tightness against in-box LOCA for JA DEMO, Fusion Eng. Des. **146** (2019) 894-897.

Maruyama, So, Fujimoto, Nozomu, Sudo, Yukio, Murakami, Tomoyuki, Fujii, Sadao, 1994. Evaluation of core thermal and hydraulic characteristics of HTTR. Nucl. Eng. Des. 152 (1-3), 183–196.

KAWAMURA, Yoshinori, NISHIKAWA, Masabumi, TANAKA, Kenichi, MATSUMOTO, Hiroyuki, 1992. Adsorption Characteristics of Water Vapor on Gamma-Lithium Aluminate. Journal of Nucl. Sci Tech. 29 (5), 436–444.

Y. Nagaya, et al., MVP/GMVP Version 3: General Purpose Monte Carlo Codes for Neutron and Photon Transport Calculations Based on Continuous Energy and Multigroup Methods, JAEA-Data/Code (2017) 2016-018.

OKUMURA, Keisuke, MORI, Takamasa, NAKAGAWA, Masayuki, KANEKO, Kunio, 2000. Validation of a Continuous-Energy Monte Carlo Burn-up Code MVP-BURN and Its

Application to Analysis of Post Irradiation Experiment. J. Nucl. Sci. Tech. 37 (2), 128–138.

Shibata, K., et al., 2011. JENDL-4.0: A New Library for Nuclear Science and Engineering. J Nucl. Sci. Tech. 48 (1), 1–30.

Schulz, B., Wedemeyer, H., 1986. PREPRARATION, CHARACTERIZATION AND THERMAL DIFFUSIVITY OF γ-$LiALO_2$. J. Nucl. Mat. 139, 35–41.

Fink, J.K., Leibowitz, L., 1995. Thermal conductivity of Zirconium. J. Nucl. Mat. 226 (1-2), 44–50.

P. Auerkari: VTT Manufacturing Technology, VTT Tiedotteita – Meddelanden – Research Notes 1792, Espoo, (1996), 14.

Faubert, Francis M., Springer, George S., 1973. Measurement of the thermal conductivity of helium up to 2100°K by the column method. J. Chem. Phys. 58 (10), 4080–4083.

Powell, R.W., Tye, R.P., Hickman, M.J., 1965. THE THERMAL CONDUCTIVITY OF NICKEL. Int. J. Heat Mass Transfer 8 (5), 679–688.

T. Otsuka, et al., T-containment performance of Li rod in high-temperature gas-cooled reactor for T production: (1) Hydrogen absorption properties of Ni coated Zircaliy-4 co-existing with Li oxide, Annual Meeting 2020 of AESJ (in Japanese).

Kleykamp, Heiko, 1999. Enthalpy and heat capacity of $LiAlO_2$ between 298 and 1700 K by drop calorimetry. J. Nucl. Mat. 270 (3), 372–375.

Chase M. W. Jr., NIST-JANAF Themochemical Tables, Fourth Edition, J. Phys. Chem. Ref. Data, Monograph **9** (1998) 1-1951.

Goto, M., et al., 2018. Nuclear and thermal feasibility of lithium-loaded high temperature gas-cooled reactor for tritium production for fusion reactors. Fusion Eng. Des. 136, 357–361.

Hatano, Y., Shimada, M., Alimov, V.Kh., Shi, J., Hara, M., Nozaki, T., Oya, Y., Kobayashi, M., Okuno, K., Oda, T., Cao, G., Yoshida, N., Futagami, N., Sugiyama, K., Roth, J., Tyburska-Püschel, B., Dorner, J., Takagi, I., Hatakeyama, M., Kurishita, H., Sokolov, M.A., 2013. Trapping of hydrogen isotopes in radiation defects formed in tungsten by neutron and ion irradiations. J. Nucl. Mater. 438, S114–S119.

Macaulay-Newcombe, R.G, Thompson, D.A, 1998. Ion beam analysis of deuterium-implanted Al_2O_3 and tungsten. J. Nucl. Mater. 258-263, 1109–1113.

Devaraj, A., et al., 2021. Neutron irradiation induced changes in isotopic abundance of ^{6}Li and 3D nanoscale distribution of tritium in $LiAlO_2$ pellets analyzed by atom probe tomography. Mater. Charact. 176, 111095.